J Electr Eng Technol.2018; 13(3): 1294-1303
http://doi.org/10.5370/JEET.2018.13.3.1294

ISSN(Print) 1975-0102
ISSN(Online) 2093-7423

Effect of Shifting the Pole-shoe and Damper-bar Centerlines on the No-load Voltage Waveform of a Tubular Hydro-generator

Zhen-nan Fan†, Li Han, Yong Liao**, Li-dan Xie**, Kun Wen*, Jun Wang*, Xiu-cheng Dong* and Bing Yao***

Abstract – This study optimises the no-load voltage waveform of tubular hydro-generators by a simple design scheme. For different centerlines of the pole shoe and damper bar, the optimisation effects on the no-load voltage waveform are investigated in two tubular hydro-generators with different weighted powers (34 MW and 18 MW). The results are compared with those of the traditional stator-slots skewed design. The quality of the no-load voltage waveform was related to the shifting degree, and the different optimisation effects between the integer slot generator (q = 2) and the fractional slot generator (q = 11/2) were analysed. This research can improve the quality of the power output and no-load voltage waveform, and provide an effective reference for improving the industrial design and manufacture level of tubular hydro-generators.

Keywords: Pole-shoe and damper-bar centerlines, Shifting, Effect, No-load voltage waveform, Tubular hydro-generator.

1. Introduction

The grid-connection security and operation of a hydro-generator largely depend on the quality of the no-load voltage waveform, which is itself influenced by the pole-shoe and damper-bar positions [1]. Especially in tubular hydro-generators, where the internal space is limited, inappropriate position of the pole shoe and damper bar will degrade the no-load voltage waveform and the electrical energy quality. Therefore, the influence of these positions on the no-load waveform must be thoroughly investigated in tubular hydro-generators.

The voltage outputs of electrical machines have been analyzed in various studies [2-13]. In an earlier study, the no-load voltage of a salient pole generator was calculated by analytical formulas [2]. More recently, the no-load voltages of electrical machines (especially hydro-generators) have been analyzed by more sophisticated techniques [3-9]. For instance, the magnetic field and harmonic voltage have been calculated and analyzed by the 2D finite-element method and the field-circuit coupling method. The influences of the damper-bar pitch and skew degree of the stator slots on generator no-load voltage have also been discussed [10-12]. In a preliminary study, no-load voltage has been analyzed in a design scheme that shifts the centerline of the damper bar [13, 14].

Simultaneously shifting the centerline of the pole shoe and damper bar (Fig.1) is a simpler and more cost-effective way of optimizing the no-load voltage waveform as compared to the traditional scheme of skewing the stator

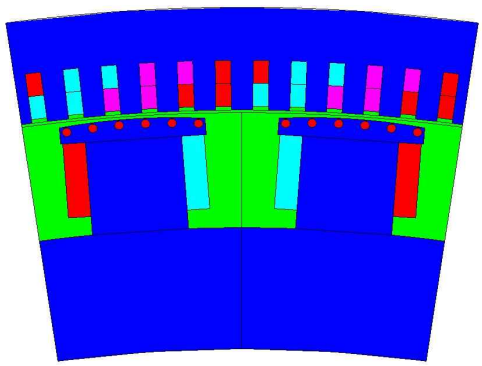

(a) No shifting the pole shoe and damper bar

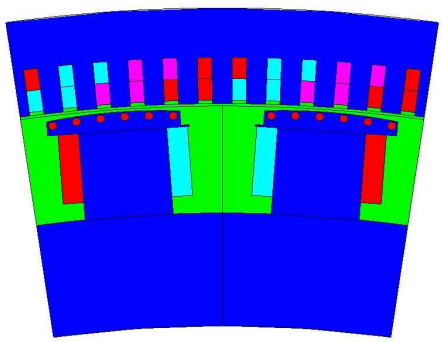

(b) Shifting centerlines of pole shoe and damper bar

Fig. 1. Shifting the centerlines of the pole shoe and damper bar

† Corresponding Author: The Key Laboratory of Fluid and Power Machinery, Ministry of Education, Xihua University, Chengdu China. (fanzhennan@126.com)
* The Key Laboratory of Fluid and Power Machinery, Ministry of Education, Xihua university, Chengdu, China. ({wkk_xhu,wangjun-xhu, sunz_xhu, yaob_xhu}@126.com)
** State Key Laboratory of Power Transmission Equipment & System security and New Technology, Chongqing University, Chongqing,. China. ({hanli_cqu,liaoyong_cqu}@126.com, 5633590@qq.com)
Received: October 7, 2017; Accepted: January 26, 2018

slot. However, this alternative design scheme has seldom been considered [15], and its effect on the no-load voltage waveform requires three directions of further study. First, the optimization effect of shifting the centerline of the pole shoe and damper bar should be analyzed over a wide, continuous range of shifting degrees. Second, the optimization effects of this design scheme should be compared between integer-slot and fractional-slot generators. Third, a more comprehensive and accurate analysis of the no-load voltage harmonics is required.

This paper analyzes the optimization effect of shifting the degree of the pole-shoe and damper-bar centerlines on the no-load voltage waveforms of two tubular hydro-generators — a 34-MW integer slot (q = 2) and an 18-MW fractional slot (q = $1^1/_2$) — to achieve the above objectives. The results are compared with those of the traditional stator-slots skewing scheme. The measures that will likely improve the quality of the no-load voltage waveform are then discussed.

2. Calculation Models

2.1 Generator parameters

The basic parameters of the integer- and fractional-slot tubular hydro-generators (of types SFWG34-44/6020 and SFWG18-68/5700, respectively) are listed in Table 1.

Table 2 clarifies the 69 design schemes applied in this study. In each design, the centerlines of the pole shoe and damper bar is shifted by a specified degree. In Table 2, t_1 is the pitch of the stator teeth, θ is the centerline shifting degree of the pole shoe and damper bar, and $\Delta\theta$ is the step length of the change in θ.

Table 1. Basic data of the two generators used in the present study

Generator type	SFWG34-44/ 6020	SFWG18-68/ 5700
Rated power P_N (MW)	34	18
Rated voltage U_N (kV)	10.5	6.3
Rated current I_N (A)	1968	1736
Rated power factor cosφ_N	0.95	0.95
Number of magnetic poles 2p	44	68
Number of damper bars per pole N_b	6	4
Slot numbers per pole per phase q	2	$1^1/_2$

Table 2. Different design schemes of the present study

Generator type	Pole shoe and damper bar shifting degree θ	Stator-slot skewing degree
SFWG34-44/6020	0–0.68t_1, $\Delta_\theta = 0.01t_1$	0
	0	0.5t_1
	0	t_1
SFWG18-68/5700	0–0.68t_1, $\Delta_\theta = 0.01t_1$	0
	0	0.5t_1
	0	t_1

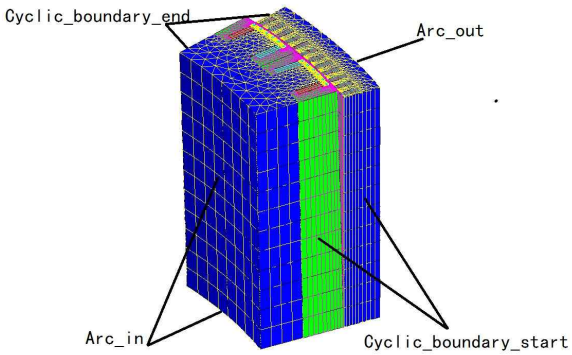

(a) Structure of stator slot skew

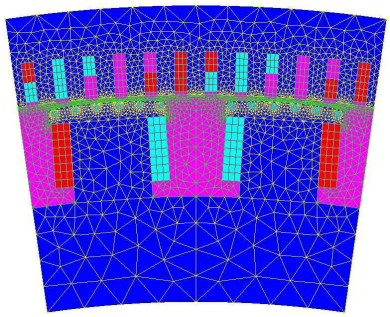

(b) Structure of the pole shoe and damper bar (no shift) with stator slot (no skew)

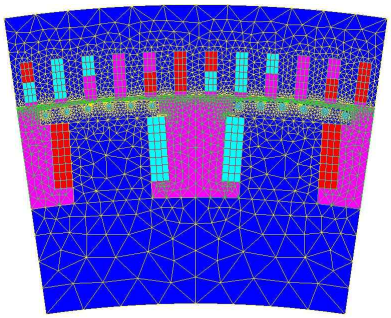

(c) Structure of the pole shoe and damper bar shifted 0.25t_1 with stator slot (no skew)

Fig. 2. Problem regions and FE meshes of electromagnetic fields

2.2 Multi-slice moving electromagnetic field-circuit coupling model of the generator

The influence of the skewed stator slot structure was analysed, with reference to the literature [19] and [20], to build up a multi-slice moving electromagnetic field-circuit coupling model of the generator.

According to the periodicity of the magnetic field, a pair of poles was chosen as the electromagnetic field calculation region. For the stator slot skewed structural design scheme, the generator was divided into twelve equal slices along the axial direction,as shown in Fig. 2(a) . For the structural schemes without the skewed stator slot, the calculation region had only one slice, which is equivalent

to a 2D electromagnetic field problem, as shown in Fig. 2(b) and Fig. 2(c).

Considering the saturation of an iron core, the 3D boundary value problem of a nonlinear time-varying electromagnetic moving field is obtained:

$$\begin{cases} \nabla\times(\nu\nabla\times\mathbf{A})+\dfrac{1}{\rho}\left[\dfrac{\partial\mathbf{A}}{\partial t}-\mathbf{V}\times(\nabla\times\mathbf{A})\right]=\mathbf{J_S} \\ \mathbf{A}\big|_{Arc\_in}=\mathbf{A}\big|_{Arc\_out}=0 \\ \mathbf{A}\big|_{Cyclic\_boundary\_start}=\mathbf{A}\big|_{Cyclic\_boundary\_end} \end{cases} \tag{1}$$

where A is the magnetic vector potential, J_s is the source current density, V is the reluctivity, V is the velocity and ρ is the resistivity.

For each slice, the current density and magnetic vector potential have only the axial z component, and the speed has only the circumferential x component. With the Coulomb norm $\nabla\cdot A = 0$ and the boundary condition of the problem region, the 2D boundary value problem of a nonlinear time-varying moving electromagnetic field for the generator is then obtained:

$$\begin{cases} \dfrac{\partial}{\partial x}(\nu\dfrac{\partial A_{slz}}{\partial x})+\dfrac{\partial}{\partial y}(\nu\dfrac{\partial A_{slz}}{\partial y})=-J_{slz}+\dfrac{1}{\rho}\dfrac{\partial A_{slz}}{\partial t}+\dfrac{V_x}{\rho}\dfrac{\partial A_{slz}}{\partial x} \\ A_{slz}\big|_{arc\_in}=A_{slz}\big|_{arc\_out}=0 \\ A_{slz}\big|_{cyclic\_boundary\_start}=A_{slz}\big|_{cyclic\_boundary\_end} \end{cases} \tag{2}$$

where V_x is the circumferential component of velocity, J_{slz} is the axial component of source current density and A_{slz} is the magnetic vector potential.

To consider the influence of the stator end winding and the rotor damper winding end rings, the coupling circuit models are established, as discussed in the literature [21-24]. The stator coupling circuit is shown in Fig. 3(a). The statorwinding parallel branch number is one, for each slice; therefore the voltage equation of the stator circuit is

$$e_s = u_{oc} + R_{1e}i_s + L_{1e}\frac{di_s}{dt} \tag{3}$$

where e_s, u_{oc} and i_s are the inductive EMF, the voltage and the current, respectively, of the stator phase winding. R_{1e} and L_{1e} are the resistance and the leakage inductance, respectively, of the stator end winding, R_L is the resistance of the load and L_L is the inductance of the loads.

Fig. 3(b) shows the circuit of damper bars in the problem region for every slice, as demonstrated previously in the literature [21], and all damper bars are connected in a cage.

Supposing that i_{k-1} and i_k are the end ring currents on the left and right branches of kth damper bar, respectively, the relationship between i_{k-1}, i_k and the current of the damper bar i_{bk} can be obtained:

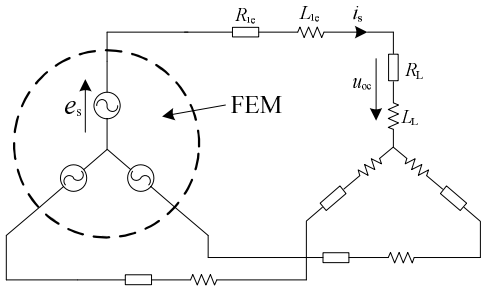

(a) Coupling circuit of the stator winding

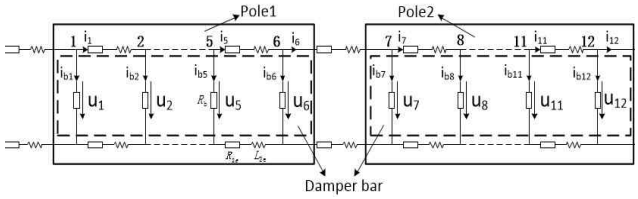

(b) Coupling circuit of the damper winding in the problem region (with two poles and all damper bars connected in a cage)

Fig. 3 Coupling circuit

$$i_k - i_{k-1} + i_{bk} = 0 \tag{4}$$

The voltage equation to describe the relationship between the kth and $(k + 1)$th branches of the damper bars is

$$u_k - u_{k+1} = 2i_k R_{2e} + 2L_{2e}\frac{di_k}{dt} \tag{5}$$

where R_{2e} and L_{2e} are the resistance and the inductance of the damper winding end ring, respectively.

From the periodic condition, the constraint conditions of the current and the voltage on the boundary are

$$i_1 + i_n + i_{b1} = 0 \tag{6}$$

$$u_n - u_1 = 2i_n R_{2e} + 2L_{2e}\frac{di_n}{dt} \tag{7}$$

where n is the number of damper bars in the problem region.

If the stator and rotor coupling circuit equations and the electromagnetic field equations are combined, the magnetic vector potential A_{slz} of slices can be calculated by the time-step FE method; then, the flux and voltage can be acquired.

Fig. 3(a) shows a simulation of the no-load operating condition of the generator when R_L and L_L are infinite. By the time-step finite element method, the no-load line voltage can be obtained as follows:

$$u_0 = \sqrt{3}(-R_{1e}i_s - L_{1e}\frac{di_s}{dt} + \frac{N_s l_{sl}}{S}\sum_{j=1}^{N_{cl}}\sum_{i=1}^{N}\left\{\iint_{S_i^+}\frac{\partial A_{slzi}}{\partial t}dS - \iint_{S_i^-}\frac{\partial A_{slzi}}{\partial t}dS\right\}) \tag{8}$$

where N_{cl} is the number of slices, N_s is the number of series conductors in the stator phase winding circuit, l_{sl} is the effective length of the stator core in a layer, S is the current area of the phase winding of each slice, S_i^+ and S_i^- are the areas of a mesh where the current inflows and outflows the winding of each slice, respectively, and A_{slzi} is the average value of the vector magnetic potential in the element.

3. Computation Results and Discussions

3.1 Quality of the no-load voltage waveform

The Chinese National Standard 1029-2005 GB/T [18] defines two parameters for no-load voltage analysis. First is the deviation of the actual from the sinusoidal waveforms of the line voltage, defined by the harmonic distortion factor (*HDF*):

$$HDF = \frac{\sqrt{U_2^2 + U_3^2 + \cdots\cdots + U_n^2}}{U_1} \times 100\% \quad (9)$$

Second is the telephone harmonic factor (*THF*), which quantifies the disturbance of voltage waveform harmonics in telecommunication.

$$THF = \frac{\sqrt{U_1^2\lambda_1^2 + U_2^2\lambda_2^2 + \ldots + U_n^2\lambda_n^2}}{U} \times 100\% \quad (10)$$

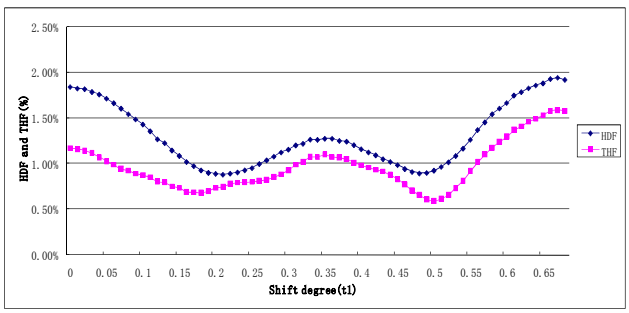

(a) SFWG34-44/6020 generator (q = 2)

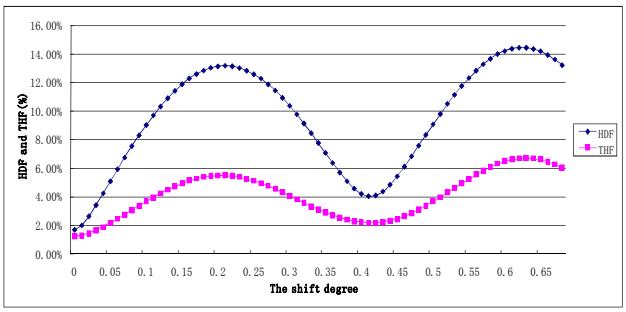

(b) SFWG18-68/5700 generator ($q = 1^1/_2$)

Fig. 4. HDF and THF versus shift of the centerlines of the pole shoe and damper bar

where U is the actual line voltage, U_i (i = 1, 2, 3 … n; n is the highest order considered) is the line voltage of the *kth* harmonic, and λ_k is the weighted coefficient of the *kth* harmonic.

As the no-load line voltages are assumed symmetric, only U_{ab} is discussed here.

Fig. 4 plots the *HDF* and *THF* versus the shift degree of the pole-shoe and damper-bar centerlines. Waveforms of the integer- and fraction-slot generators are shown in Figs. 5 and 6, respectively, and the *HDF*s and *THF*s of various design schemes are listed in Table 3.

The main results are summarized below.

In the SFWG34-44/6020 integer-slot generator with q = 2, properly adjusting the centerlines of the pole shoe and damper bar will improve the no-load voltage waveform. The improvement is especially enhanced in the ranges [0.18t_1, 0.25t_1] and [0.48t_1, 0.52t_1] of shifting degree θ.

In the SFWG18-68/5700 fractional-slot generator with $q=1^1/_2$, shifting the centerlines of the pole shoe and damper bar deteriorates the no-load voltage waveform. The deterioration is particularly severe in the ranges [0.20t_1, 0.25t_1] and [0.60t_1, 0.65t_1] of θ.

In both SFWG34-44/6020 and SFWG18-68/5700 generators, skewing the stator slots by 0.5t_1 or t_1 best improves the no-load voltage waveform. The maximum improvement is gained by skewing the stator slot by t_1.

In the SFWG34-44/6020 integer-slot generator, appropriately shifting the centerlines of the pole shoe and damper bar optimizes the quality of the no-load voltage waveform by a simpler manufacturing process than skewing the stator slot. Especially at centerline shifts of 0.21t_1 or 0.25t_1 and 0.48t_1 or 0.49t_1, the no-load voltage waveform is improved over skewing the stator slot by 0.5t_1.

Table 3. *HDF* and *THF* data for different design schemes of the two generators

Structure design scheme	*HDF* (%)		*THF* (%)	
	q = 2	$q = 1^1/_2$	q = 2	$q = 1^1/_2$
No shift of pole-shoe and damper-bar centerlines, no skew of stator slot	1.843	1.645	1.172	1.222
Pole-shoe and damper-bar centerlines shifted by 0.21t_1, no skew of stator slot	0.881	13.162	0.747	5.480
Pole-shoe and damper-bar centerlines shifted by 0.25t_1, no skew of stator slot	0.953	12.560	0.802	5.109
Pole-shoe and damper-bar centerlines shifted by 0.48t_1, no skew of stator slot	0.895	7.552	0.655	3.085
Pole-shoe and damper-bar centerlines shifted by 0.49t_1, no skew of stator slot	0.900	8.306	0.609	3.359
No shift of pole-shoe and damper-bar centerlines, stator slot skewed by 0.5t_1	1.438	1.306	0.788	1.124
No shift of pole-shoe and damper-bar centerline shift, stator slot skewed by t_1	0.475	0.767	0.238	0.436

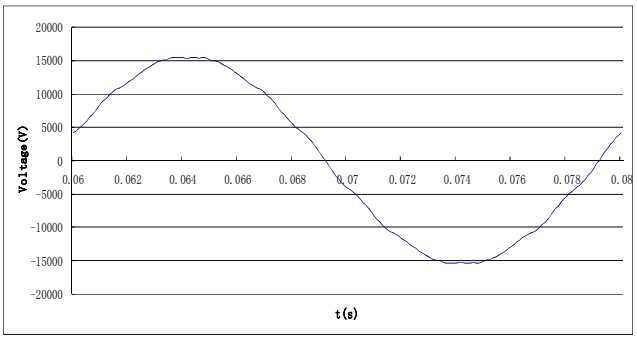

(a) No shift of pole-shoe and damper-bar centerlines, no skew of stator slot

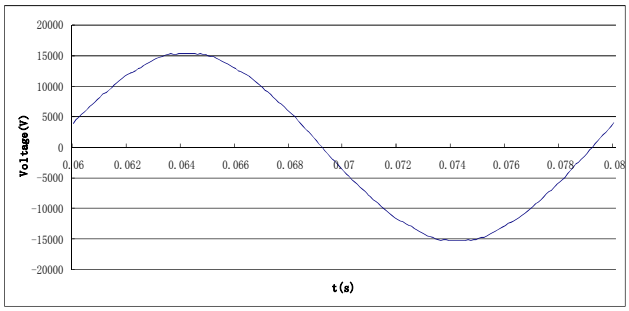

(b) Pole-shoe and damper-bar centerlines shifted by $0.21t_1$, no skew of stator slot

Fig. 5. No-load voltage waveforms of the SFWG34-44/6020 generator (q = 2)

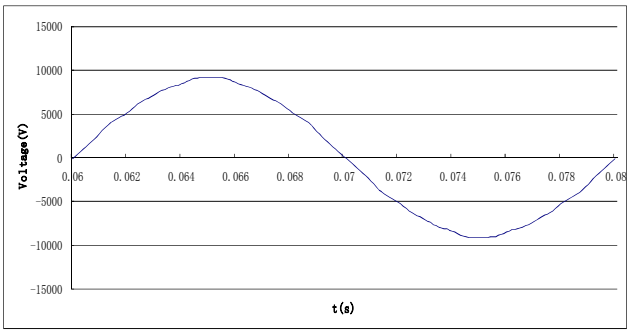

(a) No shift of pole-shoe and damper-bar centerlines, no skew of stator slot

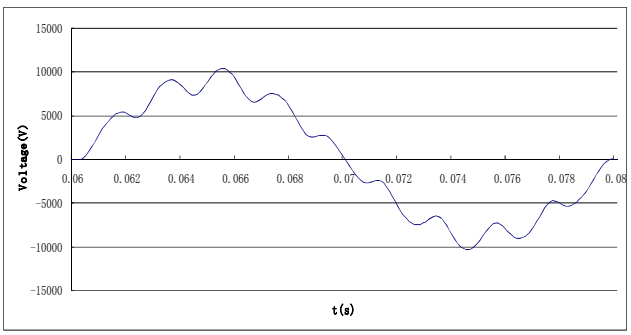

(b) Pole-shoe and damper-bar centerlines shifted by $0.21t_1$, no skew of stator slot

Fig. 6. No-load voltage waveforms of the SFWG18-68/5700 generator ($q = 1^1/_2$)

3.2 Harmonics analysis of the no-load voltage

To understand these results, we investigate the harmonics of the no-load voltage. The effects of tooth harmonics are especially important in this analysis. The ordinal number of tooth harmonics in the voltage is given by

$$\nu = k2mq \pm 1, \tag{11}$$

where k is the order of the tooth harmonics, m is the number of phases, and q is the number of slots per pole per phase. For the SFWG34-44/6020 generator with q = 2, the ordinal numbers are 11 and 13 in the first-order and 23 and

Table 4. H and T values of SFWG34-44/6020 generator (q = 2) designed by different schemes

Structure design scheme	*HDF* (%)	H (%)	*THF* (%)	T (%)
No shift of pole shoe and damper bar, no stator slot skew	1.843	1.720	1.172	0.970
Pole shoe and damper bar shifted by $0.21t_1$, no stator-slot skew	0.881	0.700	0.747	0.560
Pole shoe and damper bar shifted by $0.25t_1$, no stator-slot skew	0.953	0.770	0.802	0.610
Pole shoe and damper bar shifted by $0.48t_1$, no stator-slot skew	0.895	0.760	0.655	0.480
Pole shoe and damper bar shifted by $0.49t_1$, no stator-slot skew	0.900	0.780	0.609	0.450
No shift of pole shoe and damper bar, stator slot skewed by 0.5 t_1	1.438	1.350	0.788	0.760
No shift of pole shoe and damper bar, stator slot skewed by t_1	0.475	0.320	0.238	0.180

Table 5. Some results of H and T values of SFWG18-68/5700 generator ($q = 1^1/_2$) designed by different schemes

Structure design schemes	*HDF* (%)	H (%)	*THF* (%)	T (%)
No shift of pole shoe and damper bar, no stator-slot skew	1.645	1.30	1.222	1.180
Pole shoe and damper bar shifted by $0.21t_1$, no stator-slot skew	13.162	13.070	5.480	5.470
Pole shoe and damper bar shifted by $0.25t_1$, no stator-slot skew	12.560	12.440	5.109	5.090
Pole shoe and damper bar shifted by $0.48t_1$, no stator-slot skew	7.552	7.240	3.085	3.040
Pole shoe and damper bar shifted by $0.49t_1$, no stator-slot skew	8.306	8.020	3.359	3.320
No shift of pole shoe and damper bar, stator slot skewed by 0.5 t_1	1.306	1.280	1.124	1.090
No shift of pole shoe and damper bar, stator slot skewed by t_1	0.767	0.720	0.436	0.410

25 in the second-order tooth harmonics. For the SFWG18-68/5700 generator with $q = 1^1/_2$, the order numbers are 8 and 10 in the first-order and 17 and 19 in the second-order tooth harmonics.

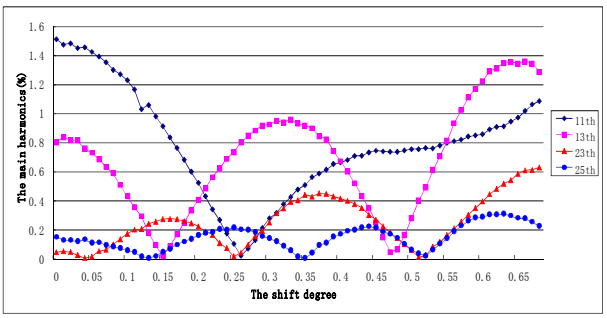

(a) SFWG34-44/6020 generator ($q = 2$)

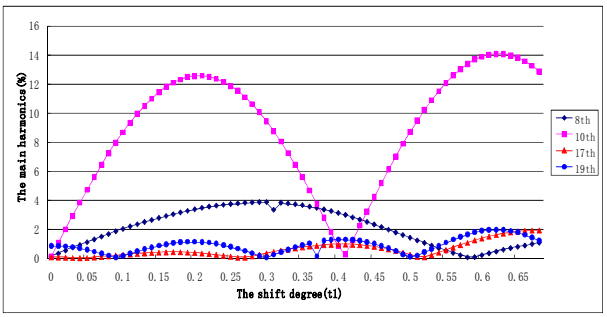

(b) SFWG18-68/5700 generator ($q = 1^1/_2$)

Fig. 7. Main no-load voltage harmonics

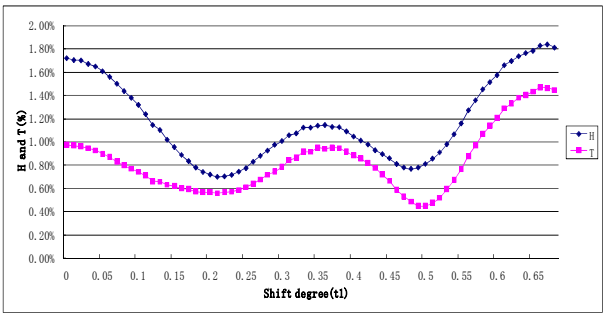

(a) SFWG34-44/6020 generator ($q = 2$)

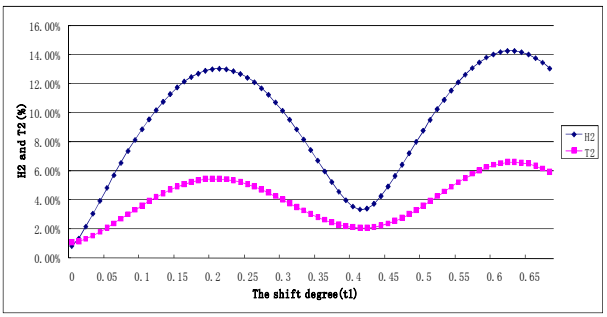

(b) SFWG18-68/5700 generator ($q = 1^1/_2$)

Fig. 8. Influence of main no-load voltage harmonics on *HDF* and *THF*

To analyze the influence of the tooth harmonics on *HDF* and *THF*, we set the *H* and *T* parameters in the SFWG34-44/6020 generator as follows.

$$H = \frac{\sqrt{U_{11}^2 + U_{13}^2 + U_{23}^2 + U_{25}^2}}{U_1} \times 100\%, \quad (12)$$

$$T = \frac{\sqrt{U_{11}^2\lambda_{11}^2 + U_{13}^2\lambda_{13}^2 + U_{23}^2\lambda_{23}^2 + U_{25}^2\lambda_{25}^2}}{U} \times 100\%. \quad (13)$$

In the SFWG18-68/5700 generator, *H* and *T* are set to

$$H = \frac{\sqrt{U_8^2 + U_{10}^2 + U_{17}^2 + U_{19}^2}}{U_1} \times 100\%, \quad (14)$$

$$T = \frac{\sqrt{U_8^2\lambda_8^2 + U_{10}^2\lambda_{10}^2 + U_{17}^2\lambda_{17}^2 + U_{19}^2\lambda_{19}^2}}{U} \times 100\%. \quad (15)$$

The main no-load voltage harmonics and representative values of the calculated parameters are shown in Figs. 7 and 8, respectively. The calculated *H* and *T* values of the SFWG34-44/6020 and SFWG18-68/5700 generators are presented in Tables 4 and 5, respectively.

From the above data, we infer the following.

In both SFWG34-44/6020 and SFWG18-68/5700 generators, the dependence of *H* and *T* on the shifting degree θ of the pole-shoe and damper-bar centerlines almost matches the responses of *HDF* and *THF* to this parameter (Fig. 2), and the *H* and *T* values are very close to *HDF* and *THF*, respectively. Therefore, the no-load voltage waveform is strongly influenced by the first- and second-order tooth harmonics.

In the SFWG34-44/6020 integer-slot generator, appropriately shifting the pole-shoe and damper-bar centerlines will effectively restrain the tooth harmonics, improving the no-load voltage waveform. For example, at shifting degrees of $0.21t_1$ or $0.25t_1$ and $0.48t_1$ or $0.49t_1$, both *H* and *T* (and consequently *HDF* and *THF*) are reduced.

In the SFWG18-68/5700 fractional-slot generator, shifting the pole-shoe and damper-bar centerlines cannot effectively restrain the tooth harmonics. Therefore, this scheme cannot improve the no-load voltage waveform. In the ranges $[0.20t_1, 0.25t_1]$ and $[0.60t_1, 0.65t_1]$ of θ, both *H* and *T* (and consequently *HDF* and *THF*) are significantly increased, so the no-load voltage waveform is badly degraded.

In both SFWG34-44/6020 and SFWG 18-68/5700 generators, skewing the stator slot by $0.5t_1$ or t_1 effectively restrains the tooth harmonics, and hence, improves the no-load voltage waveform.

3.3 Verification of the calculation

To verify the correctness of the calculation results, we

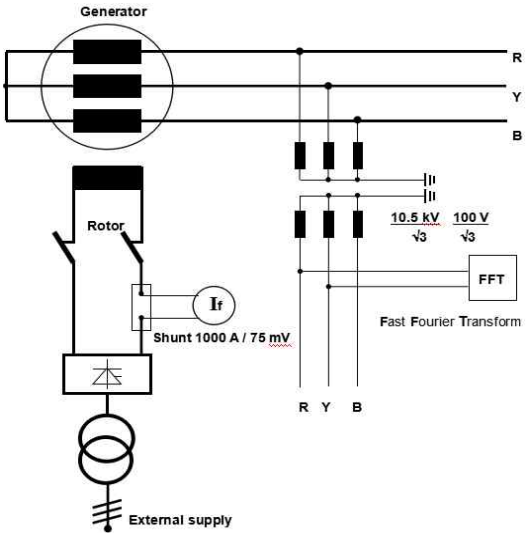

(a) Wiring diagram of the voltage waveform test

(b) The photograph of voltage waveforms test site scene

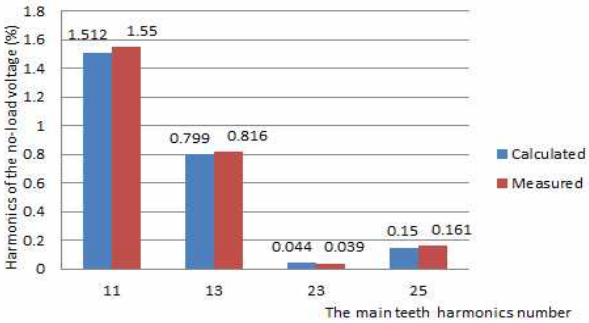

(c) Calculated and measured values of harmonics

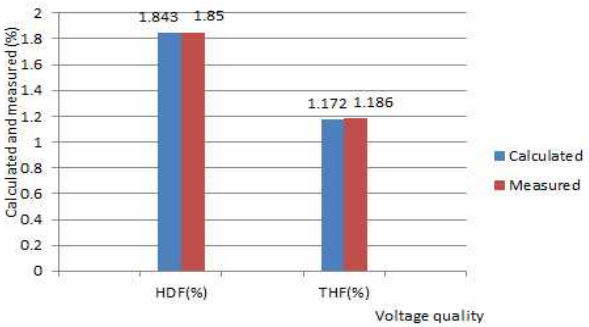

(d) Calculated and measured values of HDF and THF

Fig. 9 Test waveform and its harmonics

Table 6. Potential transformer data.

Parameter of potential transformer	Value
Rated voltage U_N (kV)	10.5
Accuracy classification	0.2
Voltage error (%)	±0.2
Phase error (')	±10
Frequency rating (Hz)	50

measure the no-load voltage in a practical SFWG34-44/6020 generator without shifting the centerlines of the pole shoe and damper bar and without skewing the stator slots.

In the no-load voltage waveform test,the sampling time is set to 0.01 ms, and the highest harmonic frequency is 5 kHz. The test wiring diagram is shown in Fig. 9(a), the photograph of voltage waveforms test site scene is shown in Fig. 9(b). The basic data of the potential transformer in the test are listed in Table 6, and the no-load voltage test and calculation values are compared in Fig. 9(c) and 9(d). The calculation and experimental results are very similar.

The no-load voltage waveforms of another SFWG45-44/5835 integer-slot tubular hydro-generator, with three slots per pole per phase (q = 3), rated power and voltage of 45 MW and 10.5 kV respectively, and seven damper bars per pole, are also calculated and verified. The results are similar to those of the SFWG34-44/6020 integer-slot generator in the present paper (Appendix).

4. Conclusion

Shifting the centerlines of the pole shoe and damper bar is a suitable technique for optimizing no-load voltage waveforms in tubular, integer-slot hydro-generators. Appropriate shifting degrees will not only restrain the tooth harmonics and effectively optimize the no-load voltage waveform but also simplify the manufacturing process and require lower-cost technology as compared to the conventional skewed stator-slot scheme. For example, in the SFWG34-44/6020 generator with q = 2, shifting the pole-shoe and damper-bar centerlines by $0.21t_1$ or $0.25t_1$ and by $0.48t_1$ or $0.49t_1$ improved the no-load voltage waveform over skewing the stator slot by $0.5t_1$.

However, this method cannot optimize the no-load voltage waveforms of tubular hydro-generators with fractional slots. For example, applying this approach to the SFWG18-68/5700 generator with q = $1^1/_2$ will seriously degrade the no-load voltage waveform.

Acknowledgements

This work was sponsored by the National natural sciences fund youth fund of China, No. 51607146 and 61703345, and the Key Scientific Research fund project of Xihua University, No.Z1520907 and Z1520909, and the

Key Research fund projects of Si chuan Provincial Education Department, No. 16ZA0155 and 16ZB0159. And this work was supported by Sichuan Science and Technology Program,No.2018GZ0391, and this work was supported by a grant from Chunhui Project Foundation of the Education Department of China,No.Z2016144. And it was sponsored by The Key Laboratory of Fluid and Power Machinery, Ministry of Education, Xihua university, Chengdu 610039, China.

References

[1] Xi-fang Chen, *Electromagnetic Calculation of Hydro-Generator*, Beijing: China Water Power Press, 2011.

[2] Zhesheng Li, "Measurement of Improving No-load Voltage Waveforms of Salient-pole Synchronous Generator", *Journal of Harbin Institute of Electrical Technology*, vol. 6, no. 3, pp.1-16, Sept 1983.

[3] Lingyun Shao, Wei Hua, Ming Cheng. "Design of a twelve-phase flux-switching permanent magnet machine for wind power generation," *in Proc*. *Electrical Machines and Systems (ICEMS)*, 2014 17th International Conference on, 2014, pp. 435-441.

[4] Wang Ting-ting, Lu Mei-ling, Zhao Xiao-Zhong, Wang Hui-zhen, Meng Xiao-li. "Magnetic field analysis and structure optimization of high speed EEFS machine," *in Proc*. *Industrial Electronics Society, IECON 2013 - 39th Annual Conference of the IEEE*, 2014, pp. 978-983.

[5] Qudsia, J., Junaid, I., Byung-Il Kwon. "Analytical analysis of the magnetic field and no-load voltage for the double sided axial flux permanent magnet synchronous generator," *in Proc*. Electromagnetic Field Computation (CEFC), 2010 14th Biennial IEEE Conference on, 2010, pp.1.

[6] Bastawade, P., Reza, M.M., Pramanik, A., Chaudhari, B.N. "No-load magnetic field analysis of double stator double Rotor radial flux permanent magnet generator for low power wind turbines" *in Proc*. Power Electronics, Drives and Energy Systems (PEDES), 2012 IEEE International Conference on, 2012, pp. 1-6.

[7] Ranlöf, M., Perers, R., Lundin, U. "On Permeance Modeling of Large Hydrogenerators With Application to Voltage Harmonics Prediction," *IEEE Trans. on Energy Conversion*, vol. 25, no. 4, pp. 1179-1186, Dec. 2010.

[8] Whei-Min Lin, Tzu-Jung Su, Rong-Ching Wu, "Parameter Identification of Induction Machine With a Starting No-Load Low-Voltage Test," *IEEE Trans. on Industrial Electronics*, vol. 59, no. 1, pp. 352-360, Jan. 2011.

[9] Bruzzese, C., Joksimovic, G. "Harmonic Signatures of Static Eccentricities in the Stator Voltages and in the Rotor Current of No-LoadSalient-Pole Synchronous Generators," *IEEE Trans. on Industrial Electronics*, vol. 59, no. 5, pp. 1606-1624, May, 2011.

[10] De-Wei Zhang, Yuan-juan Peng, Zhen-nan Fan. "No-Load Voltage Waveform Optimization and Rotor Heat Reduction of Tubular Hydro-Generator," *in Proc*. Electromagnetic Field Problems and Applications (ICEF), 2012 Sixth International Conference on , 2012, pp. 1-4.

[11] Stefan Keller, Mai Tu Xuan, Jean-Jacques Simond, "Computation of the No-Load Voltage Waveform of Laminated Salient-Pole Synchronous Generators," *IEEE Trans. on Industry Applications*, vol. 42, no. 3, pp. 681-687, May/June 2006.

[12] Zhen-nan Fan, Yong Liao, Li Han, Li-dan Xie, "No-load Voltage Waveform Optimization and Damper Bars Heat Reduction of Tubular Hydro-Generator by Different Degree of Adjusting Damper Bar Pitch and Skewing Stator Slot," *IEEE Trans. on Energy Conversion*, vol. 28, no. 3, pp. 461-469, September, 2013.

[13] Yong-gang Luo, Zhen-nan Fan. Optimization of no-load voltage waveform in a large hydro-generator by the schemes which shift the damper winding and skew stator slots. in *Proc*. EESD Conference, 2012, pp. 397-403.

[14] Hong-lian Wang, Zhen-nan Fan. No-load Voltage Waveform Optimization of Integral Number Slots Large Hydro-Generator by shift Damper winding.in *Proc*. AMSMT Conference, 2013, pp. 8-12.

[15] Guang-hou Zhou, Li Han, Zhen-nan Fan, Xiao-quan Hou, Yi-gang Liao. "No-load Voltage Waveform Optimization of Hydro-generator With Asymmetric Poles," *Proceedings of the CSEE*, vol. 29, no. 15, pp. 66-73, May 2009.

[16] Sarikhani, A., Nejadpak, A., Mohammed, O.A. "Coupled Field-Circuit Estimation of Operational Inductance in PM Synchronous Machines by a Real-Time Physics-Based Inductance Observer," *IEEE Trans. on Magnetics*, vol. 49, no. 5, pp. 2283-2286, May 2013.

[17] Youpeng Huangfu, Shuhong Wang, Jie Qiu, Haijun Zhang, Guolin Wang, Jianguo Zhu. "Transient Performance Analysis of Induction Motor Using Field-Circuit Coupled Finite-Element Method," *IEEE Trans. on Magnetics*, vol. 50, no. 2, pp. 2283-2286, Feb, 2014.

[18] Li-xin Fu, GB/T 1029-2005: The test measures of three phases synchronous machine, Bei Jing: Standards Press of China, 2012.

[19] Weilharter, B., Biro, O., Rainer, S., Stermecki, A.: "Computation of Rotating Force Waves in Skewed Induction Machines Using Multi-Slice Models," *IEEE Trans on Magnetics*, vol. 47, no. 5, pp. 1046-1049, 2011.

[20] Keranen, J., Ponomarev, P., Pippuri, J., *et al*.: "Parallel Performance of Multi-Slice Finite-Element

Modeling of Skewed Electrical Machines," *IEEE Trans on Magnetics*, vol. 53, no. 6, pp. 1204-1207, 2017.
[21] Knight, A. M., Troitskaia, S., Stranges, N., Merkhouf, A., "Analysis of large synchronous machines with axial skew, part 2: inter-bar resistance, skew and losses," *IET Electr. Power Appl*, vol. 3, no. 5, pp. 398-406, 2009.
[22] Youpeng Huangfu., Shuhong Wang., Jie Qiu., Haijun Zhang., *et al*., "Transient Performance Analysis of Induction Motor Using Field-Circuit Coupled Finite-Element Method," *IEEE Trans on Magnetics*, 2014, 50, (2), Article Sequence Number, 7021604.
[23] Sarikhani, A., Nejadpak, A., Mohammed, O. A.: "Coupled Field-Circuit Estimation of Operational Inductance in PM Synchronous Machines by a Real-Time Physics-Based Inductance Observer," *IEEE Trans. on Magnetics*, 2013, 49, (5), pp. 2283-2286.
[24] Youpeng Huangfu., Shuhong Wang., Luca Di Rienzo., Jianguo Zhu., "Radiated EMI Modeling and Performance Analysis of a PWM PMSM Drive System Based on Field-Circuit Coupled FEM," *IEEE Trans. on Magnetics*, 2017, 53, (11), Article Sequence Number: 8208804.

Appendix

For the SFWG45-44/5835 integer-slot tubular hydro-generator with q = 3, the ordinal numbers are 17 and 19 for the first-order and 35 and 37 for the second-order tooth harmonics.

Table 7 shows representative no-load voltage waveforms calculated for this generator.

The no-load voltage waveform of this generator in the $0.25t_1$-shifted scheme is presented in Fig. 10, and its harmonics are tabulated in Table 8.

Table 7. Calculated no-load voltage waveforms (U_{ab}) for the SFWG45-44/5835 generator

Schemes	Harmonics of no-load voltage (%)					Voltage quality	
	1	17	19	35	37	*HDF* (%)	*THF* (%)
No shift	100	0.30	4.90	0.09	0.11	4.926	6.489
$0.25t_1$ shifted	100	0.47	0.31	0.02	0.07	0.653	0.758

Table 8. Verification results of the no-load voltage waveform (U_{ab}) of the SFWG45-44/5835 generator in the $0.25t_1$-shifted scheme

value	Harmonics of no-load voltage (%)					Voltage quality	
	1	17	19	35	37	*HDF* (%)	*THF* (%)
Calculated	100	0.47	0.31	0.02	0.07	0.653	0.758
Tested	100	0.41	0.29	0.03	0.06	0.615	0.718

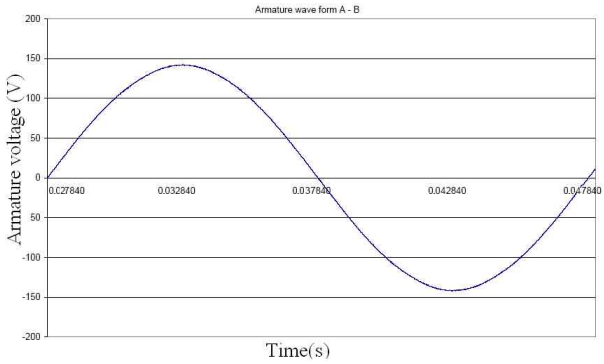

Fig. 10. No-load voltage waveforms of the SFWG45-44/5835 generator in the $0.25t_1$-shifted scheme

Zhen-nan Fan He was born in Longchang, China in 1981. He received his Ph.D. degree in electrical engineering from Chongqing University, Chongqing, China, in 2013. He is currently an associate professor at Xihua University. His research interests include magnetic and thermal field calculation of generators, electrical machinery, and motor drives.

Li Han He received the M.Sc. degree and Ph.D. degree in electrical machine from Chongqing University, Chongqing, China, in 1986 and 2008, respectively. He is currently a professor at Chongqing University. His research interests include the field calculation, the design and control of electric machines.

Yong Liao He received the M.Sc. degree in electrical machinery and the Ph.D. degree in power system control from Chongqing University, Chongqing, China, in 1988 and 1997, respectively. He is currently a professor of electrical machinery and apparatus at Chongqing University. His research interests include the magnetic and thermal field calculation of generators and the control of doubly fed electrical machines as used in renewable energy systems. In 1998, he participated in the Global Development Programme of Rockwell Automation, Milwaukee, WI. Between 2001 and 2002, he was a Visiting Professor at Norhtumbria University, U.K.

Li-dan Xie He received the M.Sc. degree in electrical engineering from Chongqing University, Chongqing, China, in 2010. He is now an engineer at Guodian Nanjing Automation Co. Ltd in China. His research interests include the field calculation of generators and renewable energy.

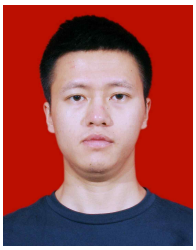

Kun Wen He was born in Chongqing, China in 1991. He is currently pursuing the M.Sc. degree at Xihua University. His research interests include magnetic and thermal field calculation of generators, electrical machinery, and motor drives.

Jun Wang She was born in Mianyang, China in 1966. She received the Ph.D. degree in electrical engineering from Southwest Jiaotong University, Chengdu, China, in 2006. She is currently a professor at Xihua University. Her research interests include magnetic and thermal field calculation of generators, electrical machinery, and motor drives.

Xiu-cheng Dong He was born in Xianyang, China in 1963. He is currently a professor at Xihua University. His research interests include the control and analysis of generators, electrical machinery, and motor drives.

Bing Yao He was born in Sichuan, China in 1981. He received the M.Sc. degree Xihua University, Chengdu, China, in 2010. He is currently a lecturer at Xihua University. His research interests include magnetic and thermal field calculation of generators, electrical machinery, and motor drives.